

SCADA Wireless Wide Area Networks

Ahmed A. A. Adas

Department of Electrical & Computer Engineering, Faculty of Engineering, KAU, P. O. Box: 80204 Jeddah, 21589, Saudi Arabia
aadas@kau.edu.sa

Abstract. A supervisory control and data acquisition (SCADA) digital wireless wide area network (DWWAN) which is adapted to power utility grid has been designed with an architecture consisting of 56 nodes (28 links) stretching over a rugged mountainous zone. Simulation is conducted for design parameters such as tower heights, total antennas per tower, path loss, rain attenuation, hop lengths and power budgets that fulfill ITU standards for availability per year. Path profiles have been simulated employing a topographic database and Global Positioning System (GPS) coordinates of the designated node sites. The radio channel is assumed as a SDH digital path employing fixed or adaptive MQAM modulation scheme with Rician fading processes. The Rician fading channel equations are established for the symbol error rate and the spectral efficiency. Such networks can deliver channel capacities up to 2×155.52 Mbit/s per single frequency pair employing co-channel double polarization (orthogonal beams) with a bandwidth of 29 MHz and a gross spectral efficiency in the range of 5-11 bits/sec/Hz. This architecture gives network operators a spectrum efficient solution and can be integrated with mobile cellular backbone networks.

Keywords: Supervisory control and Data acquisition (SCADA), Digital Wireless Wide Area Network (DWWAN), M-ary Quaternary Amplitude Modulation (MQAM), Synchronous Digital Hierarchy (SDH), Spectral Efficiency (SPE), Load Dispatch Center (LDC).

1. Introduction

A radio network consists of a group of transceivers (stations) sharing a common radio channel and communicating with each other using this channel. Each transceiver has a geographic region within which it can

communicate with other transceivers^[1]. In a multi hop DWWAN messages are transmitted via a series of intermediate transceivers to the designated nodes. Resources of the communication channel such as time, frequency, code and data link layer protocols^[2-5] are designed for the transceivers in a manner that avoids contention and provides required data rates over securely reliable links. Microwave DWWAN is very useful due to their integration with other PSTN such as cellular nets or optical networks. The Synchronous Digital hierarchy (SDH) WWAN plays a major role in various data communication requirements as backup networks across the globe, since the radio waves can cross uneven terrain with ease and can be used to set up quickly very long distance backbone links in difficult environments. The DWWAN is considered rugged and provide good availability during natural catastrophes.

Since DWWAN channels (with frequencies in the range 2-60 GHz) can be assumed as line of sight (LOS) microwave fading channels^[6], the statistical characteristics of the fading channel can use the Nakagami-m distribution model^[7]. However Turin^[8] and Suzuki^[9] have shown that Nakagami-m distribution is best fit for data signals received in urban radio mutlipath channels. In LOS microwave fading channels the Rician (Rice distribution or Nakagami-n distribution) fading model^[10] has been confirmed experimentally by Rummler^[11]. The Rice fading distribution function is integrated with the DWWAN simulation model. These channels are assumed to operate employing adaptive or fixed MQAM modulation schemes at the physical layer level. Equations for the MQAM Rician faded Symbol Error Rate (SER) and spectral efficiency in units of (bits/sec/Hz) is established. The ITU link design parameters are simulated for the 56 nodes WWAN architecture. These 56 nodes with 28 links are superimposed on a large power grid.

The utilization of SCADA^[12,13] in power systems management is necessary to achieve grid management as well as control of complex dynamic variations such as load changes, protective relaying of power links, fault isolation, generation telecontrol, remote video transmission and telemetry covering all parameters of power generation, distribution and security. The outlined model for wireless wide area networks is interfaced with generation plants and distribution substations that cover a large rugged mountainous zone.

2. DWWAN Architecture

The structure of the DWWAN is superimposed on the power grid that covers a rectangular area in Aseer Region of Saudi Arabia [(17° 36' N) to (18° 32' N)] latitude and [(42° 20' E) to (43° 40' E)] longitude. The topography of the region is very rugged with mountain heights reaching to 3130 meter above sea level. A total of 56 nodes (28 links) exist in the network. The various node pairs are named (jA,jB) with links (L_j) for j=1,2,...28, *i.e.* {L₁(1A,1B),...L₂₈(28A,28B)}. These wireless nodes are superimposed on the locations of the various substations, power stations and the central power stations. The DWWAN has been designed to provide high quality radio transmission links meeting the synchronous digital hierarchy (SDH) standards transmitting multimedia packets and is compatible with the optical ground wire (OPGW) network ^[12] that can be attached to the high tension grid. This architecture provides dual or tandem highly reliable routes for the utilities. The architecture of integrating the DWWAN with the power grid is shown in Fig. 1, in which the central microwave station is attached to a cluster of processors forming the Load Dispatch Center (LDC). While microwave outstations are connected to the SCADA remote terminal units (RTUs) which are connected to either the power plants, or substations. The DWWAN in the physical layer employs the MQAM modulation scheme ^[6,10] for the RF signals in order to achieve high spectral efficiency for broadband data communication. The network can be configured in point to point transmission architecture (from the central station to the outstation or repeater) or point to multi-point (from the central station to multi-outstations or repeaters) as indicated in Fig. 2. The various SCADA remote stations collect the various grid parameters and sending them to the load dispatch center (LDC) processors on 24 hours basis, daily all year round. Any mobile cellular backbone may interface to the DWWAN ^[14,15].

3. SCADA Systems

The main drawback when using power line carrier communication for power protective relaying is that a fault that causes a relay operation can also cause a loss of communication signal when it is needed most. Normally utilities provide a backup relay set and another communication network {such as the DWWAN under consideration or optical network ^[12]} for critical relay applications. The SCADA network attributes are shown in Fig. 2, with the dispatch load center (DLC) processors. The key elements are:

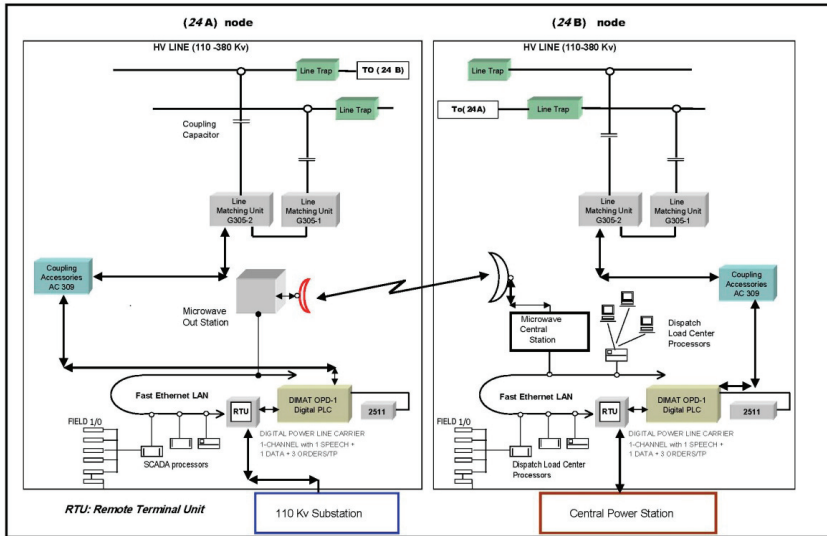


Fig. 1. The architecture of the digital wireless wide area network (DWWAN) integrated with the power grid.

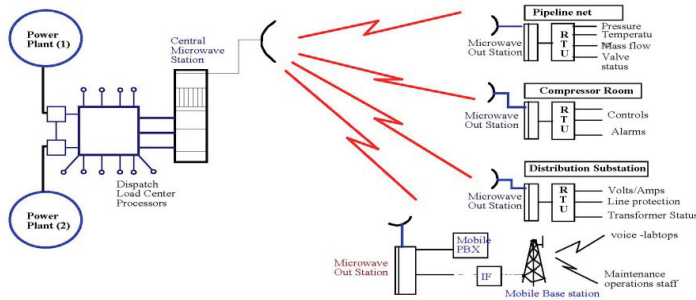


Fig. 2. The SCADA-DWWAN architecture provides communication for the power utilities.

3.1 Remote Terminal Units (RTUs)

These are special purpose computer stations with many digital inputs (status) /outputs (controls) and AD/DA converters. These processors are rugged and fully protected against spurious electrical transients. They are manufactured according to the IEEE-472 and ANSI C37.90a surge withstands capability (SWC) [13] (5kv). Any RTU may have multiple communication ports, enabling networking with a single master server processor or as part of a LAN or WAN. There are many RTU types among them (A) *Transmission Substation RTUs*: These are

large systems deployed at 380Kv-110 kV substations and power generation plants, where a large number of control and data points are required. Each RTU may employ multiple processor cards and has a distributed input/output (I/O) design, in which I/O modules are connected to data highways which loops through the substation. These RTUs have the ability to interface with other substation intelligent electronic devices (IEDs). These devices such as current/voltage/power meters, relays, reclosers, voltage regulators, and tap position indicators, are interrogated by the RTU, which reports the status information from these devices back to the master servers in the SCADA network. (B) *Distribution Substation RTUs*: These are smaller RTUs and are used across the power grid various distribution substations (69-13 kV) or utility poles. They are used to control remote switches and capacitor banks on the high voltage lines. On monitoring status variables and automating feeders and on underground or above ground networks covering the whole power distribution network in urban or rural areas. Typically each RTU has a single or multiple board processors that have all digital I/O, the system is built to be rugged and have integrated data communication modules. They utilize digital signal processing to perform fault detection/isolation on the power grid or calculate electrical parameters.

All kinds of RTUs use programmable logic controllers (PLC) which have been used extensively in process industries and now are used to implement relay and control in power substations. The control outputs can be manipulated locally or from the computer servers at the dispatch load centers. In addition RTUs have electrical transducers which in effect analog computers that measures watt, var, watt/var, watt/watthour, var/varhour, voltampere, voltamperehour, current, voltage, phase angle, voltage angle, frequency, temperature, dc isolation, and signal conditioning. Intelligent electronic devices (IED) are employed to condition and preprocess transducer inputs for the RTUs.

4. Synchronous Digital Hierarchy (SDH) Radio Link Model

Radio frequency signals are susceptible to propagation anomalies such as multipath propagation fades for long distance links and fading due to precipitation. The ITU-T G.826 & ITU-R P.530 ^[16,17] models define four error performance events for SDH-WWAN links, these are (1) *Errored Block (EB)*: A block of data in which one or more bits are in error. (2) *Errored Second (ES)*: A one second period with one or more

errored blocks. (3) *Severely Errored Second (SES)*: A one second period which contains ($\geq 30\%$) errored blocks or at least one defect. The SES is a subset of ES. (4) *Background Block Error (BBE)*: An errored block which is not occurring as part of the SES event. These four events are translated into three error performance parameters, namely (A) *Errored Seconds Ratio (ESR)*: The ratio of ES to total seconds in link available time (normally taken as the worst month period of the region climate). (B) *Severely Errored Second Ratio (SESR)*: The ratio of SES events to total seconds in link available time. (C). *Background Block Error Ratio*: The ratio of BBE to total blocks transmitted in available time. The count of total blocks excludes all blocks during SES events.

In addition ITU-T G.826 ^[16] considers unavailable time as the accumulation of all Severely Errored Seconds (SES) states lasting longer than 10 consecutive seconds. The parameter SESR is the ratio of the accumulation of all SES states lasting less than 10 consecutive seconds divided by the available time. It is assumed that rain fades will always last longer than 10 consecutive seconds and therefore rain fades are classified as unavailability. ITU-R P.530-8 ^[17] standard states that multipath fades will always be less than 10 consecutive seconds and therefore will be classified as severely errored seconds (SES). Alternatively the SESR is the worst month multipath fade probability at the BER_{SES} receiver threshold. Under this definition rain fades are assigned to unavailability and multipath fades are assigned to SESR. If (P) stands for measurement period (normally the worst month of the region climate) and (UAS) is the total unavailable seconds during the (P) period (unavailable time of the link). The equations which describe the above three parameters ^[17,18] for multipath fades are:

$$BBER = \frac{\sum_{i=1}^q (BBE)_i}{[(P - UAS) - \sum_{j=1}^r (SES)_j]n} = \int_{BER_A}^{BER_B} w_{BBER}(x)g_{BER}(x)dx \quad (1)$$

$$SESR = \frac{\sum_{j=1}^r (SES)_j}{[(P - UAS)]} = \int_{BER_A}^{BER_B} w_{SESR}(x)g_{BER}(x)dx \quad (2)$$

$$ESR = \frac{\sum_{k=1}^v (ES)_k}{[(P - UAS)]} = \int_{BER_A}^{BER_B} w_{ESR}(x)g_{BER}(x)dx \quad (3)$$

where $w_{abcd}(x)$ represents the relationship between (SESR, BBER, ESR)

and the bit Error rate (BER) of the digital channel, while $g_{BER}(x)$ is the pdf of BER. The integration limits typical interval is $\{BER_A = 1E-03, BER_B = 1E-12\}$. The parameter (n) is the number of blocks/sec., which can be either $\{(n = 8000 \text{ blocks/sec ITU-R P.530}), N_B = 19940 \text{ bits/block}\}$ or $\{\text{ITU-R G.829}, n=192000 \text{ Blocks/sec}, N_B=810 \text{ bits/Block}\}$. The unavailability due to rain can be evaluated in the worst month $\{\text{of the region climate}\}$ at the BER_{SES} receiver threshold level and this will be SESR (rain). The other two parameters BBER (rain) and ESR (rain) can be evaluated using equations (2) and (3)^[17,18].

The ITU-R P. 530-10^[18] propagation model with PATHLOSS software system^[19], has been utilized in the DWWAN simulations with C++ modules that has been developed for MQAM Rician fading channel. The various links in the DWWAN model is covered by the following digital RF channel^[10] equations:

$$(C_R / N)_{RX} = P_T + \alpha_{fs} + G_{TX} + G_{RX} - k_b T - B - F_N - L_m = \left(\frac{E_b}{BN_0} \right)_{Faded} \cdot R_{b(datarate)} \quad (4)$$

$$LinkMar(LM) = (C_R / N)_{RX} - FadingMar(\xi) - RXsensitivity_{requiredBER} \quad (5)$$

$$\alpha_{fs} = 20 \log_{10} \left(\frac{\lambda}{4\pi d_{ij}} \right) \quad (6)$$

$$(P_{error-MQAM})_{unfaded-channel} = P_{\sqrt{M}}(2 - P_{\sqrt{M}}) \quad , \quad M = 2^m \quad (7)$$

$$P_{\sqrt{M}} = 2 \left(1 - \frac{1}{\sqrt{M}} \right) Q \left[\sqrt{\frac{3\bar{E}_S}{(M-1)N_0}} \right], \quad \langle \gamma \rangle = \bar{\gamma} = \frac{\bar{E}_S}{N_0} = m\gamma_b \quad , \quad \gamma_b = \left(\frac{E_b}{N_0} \right) \quad (8)$$

$$Q(x) = \frac{1}{2} \text{erfc}(x / \sqrt{2}) \quad (9)$$

where equation (4) is the Carrier to noise ratio at the receiver with $\{P_T =$ transmitted power, $\alpha_{fs} =$ free space loss, $G_{pq} =$ gain of transmitter (TX) or receiver (RX), $k_B =$ Boltzmann's constant, $T =$ noise temperature, $B =$ bandwidth, $F_N =$ noise figure, $L_m =$ other losses, $E_b =$ energy per bit, $R_b =$ data rate $\}$. The probability of error in the uncoded digitally transmitted MQAM constellation of signals in additive white gaussian channel (AWGN), for coherent detection is given by equations (7) and (8)^[10]. Noting that (M) is number of symbols in the MQAM modulation and (m) is the number of bits per symbol, and equation (8) is exact when (m) is even. $\langle \gamma \rangle$ is the average symbol signal to noise ratio (SNR), and γ_b is the SNR per bit.

4.1 Adaptive MQAM Rician Fading Channel

Assuming the wireless RF channel as a frequency non-selective slowly fading channel ^[10], Let (SER) be the target symbol error rate probability for the digital link, which operates at the average received signal to noise ratio (\bar{E}_S/N_0), where \bar{E}_S is the average received energy per MQAM symbol and (N_0) is the noise density. Let the instantaneous received signal power per symbol as (γ). Since each MQAM constellation has Nyquist data pulses with duration of T_S ($B=1/T_S$), if

$$\bar{E}_S / N_0 = S_{av} T_S / N_0 = \langle \gamma \rangle = m \langle \gamma_b \rangle \quad (10)$$

(S_{av}) is the average power then the average $\langle E_S \rangle / N_0$ equals the average SNR, *i.e.*:

The Rician pdf ^[10] signal power can be written in terms of the average symbol SNR $\langle \gamma \rangle$ and the instantaneous SNR per symbol (γ) as:

$$pdf(\gamma)_{Rician} = g_P(\gamma) = \frac{(1+K)}{\bar{\gamma}} e^{-K} \exp\{-(1+K)\gamma/\bar{\gamma}\} I_0\left\{\sqrt{\frac{4K(K+1)\gamma}{\bar{\gamma}}}\right\} \quad (11)$$

Where (K) is the Rician factor {defined as ratio of the signal power in the specular line of sight (LOS) component to the local mean scattered random power component}, and $I_0(x)$ is the modified Bessel function of zero order.

Since the spectral efficiency scheme equals the data rate per unit bandwidth, *i.e.* $SPE = (R_{b(\text{data rate})} / B)$. Then for fixed M symbols, $R_{b(\text{data rate})} = (\log_2 M) / T_S$, so the spectral efficiency (SPE) in bits/sec/Hz for fixed M-QAM modulation is $\log_2 M$, the number of bits per symbol. This efficiency depends on the average transmitted power and the SER of the MQAM modulation. Equations (7) & (8) give the unfaded BER for an AWGN channel with MQAM modulation and ideal coherent detection. By using the expansion of $\text{erfc}(x)$, and large signal to noise ratio E_S/N_0 , equations (7) & (8) can be approximated as:

$$P_{eMQAM-unfaded} \approx 2\left(1 - \frac{1}{\sqrt{M}}\right) \text{erfc}\left[\sqrt{\frac{3\bar{E}_S}{2(M-1)N_0}}\right] \cong 2\sqrt{\frac{2(M-1)N_0}{3\pi\bar{E}_S}} \exp\left(-\frac{3\bar{E}_S}{2(M-1)N_0}\right) \quad M \geq 4 \quad (12)$$

In a fading channel with nonadaptive transmission (constant power & rate), the received SNR varies with time. Fading is approximated as a discrete-time finite state Markov process^[20] with time discretized to the symbol period T_s . In this Markov process (γ) remains within one region over a symbol period, and from a given region, the process can only transit to the same region or to adjacent regions. For the fixed modulated radio channel which is subjected to Rician fading, one can assume that (γ) stays within one region over the period (T_s). The average MQAM symbol error rate probability (SER) over the fading channel is obtained by integrating the probability equation (12) over the Rician fading distribution $g_P(\gamma)$ of equation (11). Thus

Using the closed form integral number 6.618-4, p.711 in^[21], taking θ , Φ and Ψ as general constants. The exact solution to equation (13) becomes:

$$SER_{MQAM-faded} \leq \int_0^{\infty} P(\gamma) e_{MQAM-undefaded} g_P(\gamma) d\gamma \tag{13}$$

$$P_{eMQAM}(K, \bar{\gamma}, M) \leq 2\theta \int_0^{\infty} \exp(-\Phi x^2) I_0(\Psi x) dx$$

$$P_{eMQAM}(K, \bar{\gamma}, M) = \theta \sqrt{\frac{\pi}{\Phi}} \exp\left(\frac{\Psi^2}{8\Phi}\right) I_0\left(\frac{\Psi^2}{8\Phi}\right) \tag{14}$$

$$\Psi = \sqrt{\frac{4K(1+K)}{\bar{\gamma}}} \quad , \quad \Phi = \{3/2(M-1)\} + \{(1+K)/\bar{\gamma}\}$$

$$\theta = 2\sqrt{\frac{2(M-1)}{3\pi}}(1+K)\frac{e^{-K}}{\bar{\gamma}}$$

Equation (14) gives the symbol error rate probability $p_e(K,\gamma,M)$ for Rician MQAM channels and is plotted in Fig. (3) for the two sets $\{M=4, K=10, 15, 20 \text{ dB}\}$ and $\{M=256, K=5, 10, 20 \text{ dB}\}$. Clearly to maintain a target SER, if we increase the number of symbols M form 4 to 256 we must increase $\langle\gamma\rangle$. Without power adaptation by the transmitter (fixed M) and fixed data rate, the spectral efficiency for fixed ($M=4$) is $\{\log_2 M = 2 \text{ bits/s/Hz at BER of } 1.8E-06\}$ for $K=10$, and $\langle\gamma\rangle=24 \text{ dB}$, clearly using higher (M) values will give higher spectral efficiency (SPE) $\{\text{at } (M=256, \text{SPE}= 8 \text{ bits/s/Hz}), (M=512, \text{SPE}=9), (M=2048, \text{SPE}=11), \text{etc.}\}$. From Fig. 3, as well, it is clear that for fixed (M) as the Rician K factor

increases, less power is needed in order to achieve the same SER. This happens because as (K) increases the fading depth decreases.

If a variable data rate, variable power adaptive MQAM scheme is employed [20]. We consider adapting the transmit power $S(\gamma)$ relative to γ , subject to the average power constraint S_{av} . The received SNR is then $[\gamma \cdot S(\gamma)/S_{av}]$ and $[\{ \langle E_S \rangle / N_0 \} = \{ S_{av} T_S / N_0 \} = \langle \gamma \rangle]$, taking the BER bound for each value of (γ) as $BER(\gamma)$, and the number of symbols $M(\gamma)$, then from [20], the BER for an AWGN channel with MQAM modulation and ideal coherent phase detection is tighter bounded to an approximation which is good to within 1dB for $M \geq 4$ and $0 \leq \langle \gamma \rangle \leq 30$ dB.

$$BER(\gamma) \leq 0.2 \exp \left[\frac{1.5\gamma}{M-1} \frac{S(\gamma)}{S_{av}} \right] \quad (15)$$

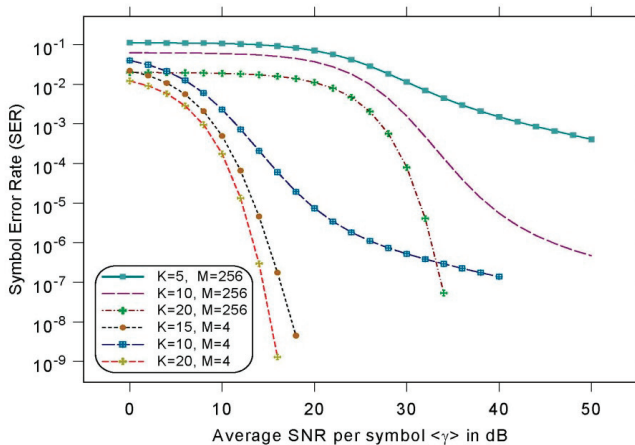


Fig. 3. The SER for MQAM Rician fading channels, two sets are plotted; $\{M=256, K=5, 10, 20\}$ dB and $\{M=4, K=10, 15, 20\}$ dB.

By arranging equation (15) and adjusting M and $S(\gamma)$ to maintain a fixed BER yields the following maximum constellation size for a given BER:

$$M(\gamma) = 1 + \frac{1.5\gamma}{-\ln(5BER)} \frac{S(\gamma)}{S_{av}} \quad (16)$$

$$\langle \log_2 M(\gamma) \rangle = \int \log_2 \left(1 + \frac{1.5\gamma}{-\ln(5BER)} \frac{S(\gamma)}{S_{av}} \right) g_P(\gamma) d\gamma$$

By maximizing equation (16) we are maximizing the spectral efficiency, since we indicated previously that $\log_2(M)$ is the spectral efficiency (SPE) in bits/sec/Hz, equation (16) is subject to the power constraint and the optimal power control policy^[24] given by:

$$S_{av} = \int S(\gamma)g_p(\gamma)d\gamma$$

$$\{S(\gamma)/S_{av}\} = \begin{cases} (1/\gamma_0)-(1/\gamma Z), & \gamma \geq \gamma_0 / Z \\ 0, & \gamma < \gamma_0 / Z \end{cases} \quad (17)$$

Where $(\gamma_0/Z=\gamma_z)$ is the optimized cutoff fade depth and $(Z=\{1.5/\ln(5BER)\})$. By employing equations (11), (17) into equation (16), we obtain the maximum spectral efficiency (SPE_{max}) for the uncoded adaptive MQAM over Rician fading channel as:

$$SPE_{max} = \left(\frac{(1+K)e^{-K}}{\bar{\gamma} \ln(2)} \right) \int_{\gamma_z}^{\infty} I_0 \left(\sqrt{\frac{4K(K+1)\gamma}{\bar{\gamma}}} \right) \cdot \exp \left(-(1+K)\frac{\gamma}{\bar{\gamma}} \right) \cdot \ln(\gamma/\gamma_z) d\gamma \quad (18)$$

Where γ_z is the cutoff fade depth, noting that equation (18) gives the spectral efficiency for Rayleigh distribution when $K=0$, { Rayleigh distribution is frequently used to model mutlipath fading with no direct line of sight (LOS) path}. Looking into equations (17) & (18), clearly the $0 \leq K \leq \infty$

$$\gamma_z = -(\gamma_0 / 1.5) \ln(5BER)$$

spectral efficiency for the uncoded adaptive MQAM has an effective power loss of (Z) relative to the optimal transmission scheme. Equivalently (Z) can be considered as the maximum coding gain for the adaptive MQAM scheme^[20]. Simulation of equation (18) is plotted in Fig. 4 for the BER values of $\{10^{-3}, 10^{-6}, 10^{-9}, K=10 \text{ dB}\}$ versus the average MQAM symbol SNR $\langle \gamma \rangle$ and compared with the Shannon limit^[10]. The plot clearly shows that the spectral efficiency reduces at lower values of the BER for the digital link. For data communication the suitable level is $BER=1E-06$ and this will give SPE_{max} in the range of $\{2-9 \text{ bits/sec/Hz}\}$ for $\langle \gamma \rangle$ in the interval of $\{12-32 \text{ dB}\}$. Clearly adaptive modulation is superior to fixed modulation in terms of power conservation, if the channels are severely faded $\{K \text{ decreases}\}$ $\{\text{as in Fig. 5}\}$ Then the required power is increased to maintain the target SPE_{max} , SER & BER. However if fading decreases, then (K) increases and the required power to attain the target SPE_{max} , SER & BER is reduced.

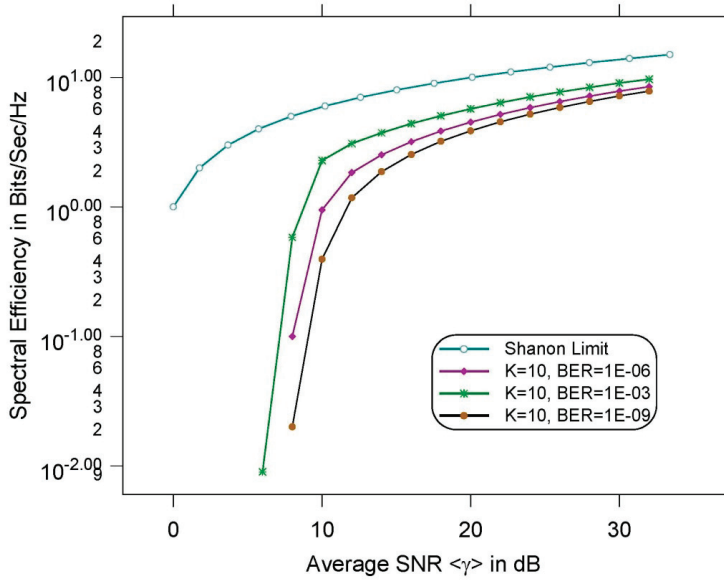


Fig. 4. SPE for Adaptive MQAM in Rician fading channels with K constant and BER varying.

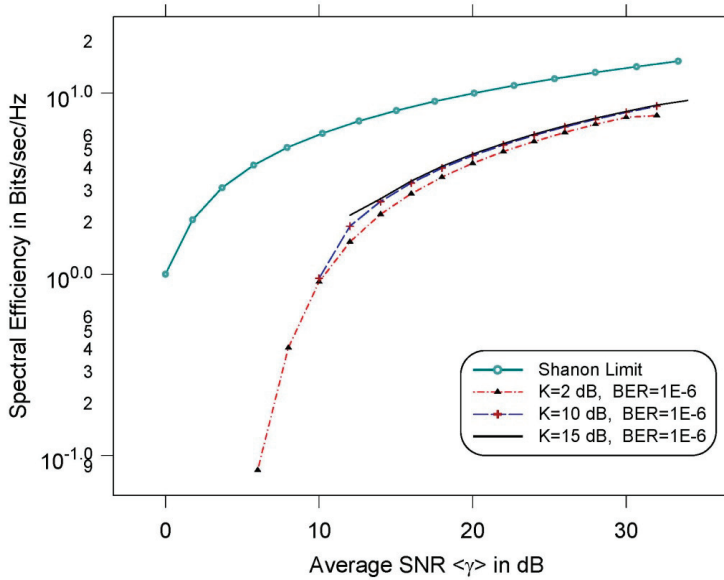


Fig. 5. SPE for adaptive MQAM Rician fading channels with BER constant and K varying.

4.2 Radio Link Error Performance & Availability Objectives

We assume that the required BER= 10^{-6} for all the links as they are used for multimedia data communication. The digital radio link which implement adaptive or fixed MQAM modulation, error correction codes and equalizers, tend to produce clusters or bursts of errors {a burst of error is defined as a sequence of errors which starts and ends with an errored bit such that the time between two errors is less than the memory of the system.}^[16]. Typical values for high level modulation such as MQAM are (10-20%) errors per burst, and the burst may contain several blocks. The SDH link prediction methods are based on the assumption that BER, which is the fundamental parameter of existing prediction methods, is related to the error performance parameters SESR, BBER and ESR. For STM-1 signals ITU-R P.530-8 defines {STM-1 data rate = 155.52 Mbits/sec, [BER_{SES} = $2.3 \times 10^{-5} \times \beta$], where ($\beta=1$) indicates a Poisson distribution of errors, the number of Blocks/sec (n) = 8000, the number of Bits/Block (N_B) = 19940}. SDH links as well might be designed according to ITU-R G.829 which defines {(BER_{SES} = ($1.3 \times 10^{-5} \times \beta$) + (2.2×10^{-4}))} with $n=192000$ Blocks/Sec, and $N_B = 801$ Bits/Block}. ITU-T G.826^[20] outlines typical values for SDH links as {over 27500 Km path (SESR = 2.0×10^{-3} , ESR = 16.0×10^{-2} and BBER = 2.0×10^{-4}) for data rates > 55 to 160 Mbits/Sec}. Thus SESR, BBER, and ESR performance parameters are essential in any SDH digital links prediction, they can be evaluated using the integral equations of (1), (2) & (3), the SDH central and out stations signature and the region climate. The approximation technique of the ITU-R P.530.8^[17] has been employed in evaluating equations (1), (2) and (3) for all the 28 links under consideration. The SESR, BBER, ESR for the 28 links covering multipath fades are simulated in Fig. 6 (a) & 6 (b) and compared with the ITU G.826 target. On the average each link has {SESR = 3.3×10^{-6} , BBER = 5.1×10^{-6} , & ESR = 16×10^{-6} }, while the ITU G.826 target in the average for each link SESR is {SESR (ITU) = 16×10^{-6} }, clearly all the links fulfill the ITU requirements. Noting that for large fade margins rain fades are assigned to unavailability and multipath fades are assigned to SESR^[16]. Since as well multipath fades lasting longer than 10 consecutive seconds were assigned to unavailability of the link according to ITU G.826^[16]. The unavailability probability per link^[16-18] and the total unavailable time per year are plotted in Fig. 6 (c) .It shows that on the average each link will be out for about 9 minutes per year, and the

whole {56 nodes, 28 links} DWWAN architecture has an availability of about 99.83% per year.

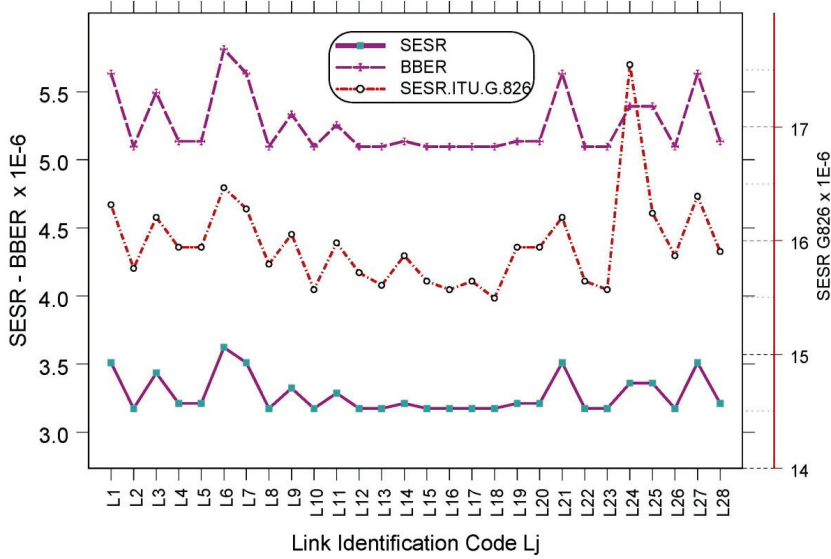


Fig. 6 (a). Simulated digital links parameters showing severely errored seconds ratio (SESR), background block error ratio (BBER) and SESR ITU G.826 standard per link.

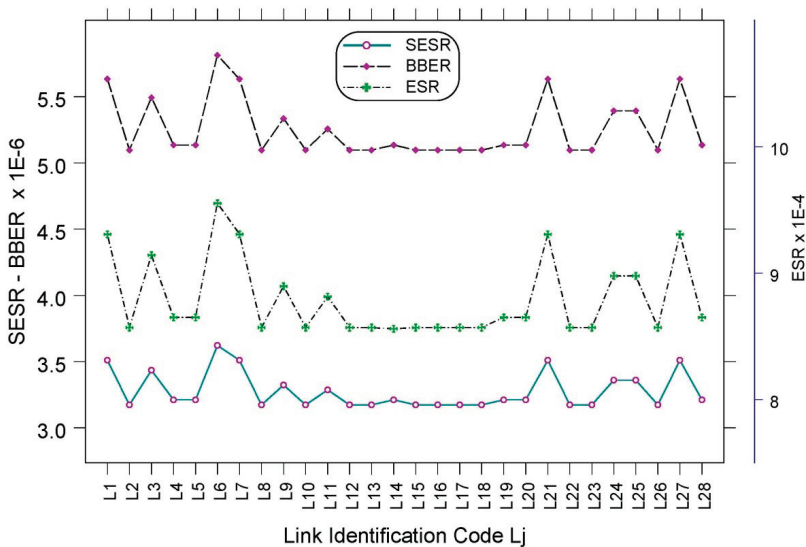


Fig. 6 (b). The SDH-DWWAN link performance parameters showing SESR, BBER and ESR per link.

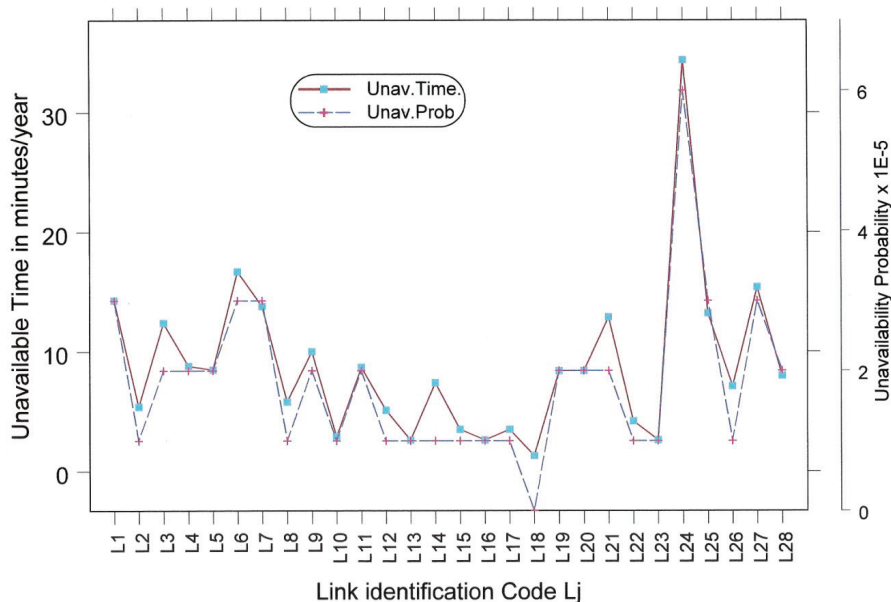


Fig. 6 (c). The unavailable time per link per year and the unavailability probability, noting that L24 is the longest hop (53.44 km).

4.3 Comparison of Rain Attenuation Models

Radio links are subjected to rain induced attenuation due to absorption and scattering, especially if the RF carrier wavelength is close to the diameter of the rain droplets. This attenuation increases the overall path loss, limits the coverage zones and consequently degrades the network performance. Extensive analysis of rain effects on the propagation of electromagnetic waves have been published in the literature [22-25]. The ITU model for the computation of rain effects is based on the ITU-R.P.530 for terrestrial networks [17,18]. There is another widely used model known as the “Crane model”, after R. K. Crane [26]. The Crane prediction model, which is based on the (aR^b) rain attenuation formula, where (R) is the point rain rate in mm/hr. The constants “a” and “b” are rain attenuation coefficients, which are functions of frequency and polarization and are tabulated by Olsen [27].

Another empirical rain attenuation model, which is based upon nominal H₂O droplet sizes and distribution, facilitates computations of attenuation rate $(AR)_{\text{rain}}$ in (dB/km) due to a specified rainfall rate. This model is referred to as the Simplified Attenuation Model (SAM/CCIR) [28].

The above three models are simulated for the DWWAN under consideration (using hop lengths of 2 & 53.5 km) in Fig. 7, showing that for the DWWAN, it is appropriate to operate below the 10 GHz frequency for the RF carrier. At the selected frequency of 4 GHz, with rain rate 15 mm/hr Crane model gives an average attenuation of 0.0229 dB/km, while the SAM model gives 0.0141 dB/km. The ITU-R.P530 model^[17,18] for rain attenuation gives about 0.01086 dB/km at (4GHz & R=15 mm/hr (V)). The three models in Fig. 7 are showing that up to 10 GHz all the models are nearly equal in predicting average rain attenuation, as these bands have long propagation distances. Such bands are only mildly affected by rain but they tend to bounce and result in a high amount of multipath propagation. However for carrier frequencies in the range of 11-80 GHz, the ITU-RP530 model generally gives lower attenuation (for Rain rate R=15 mm/hr (V)), than the SAM or Crane models.

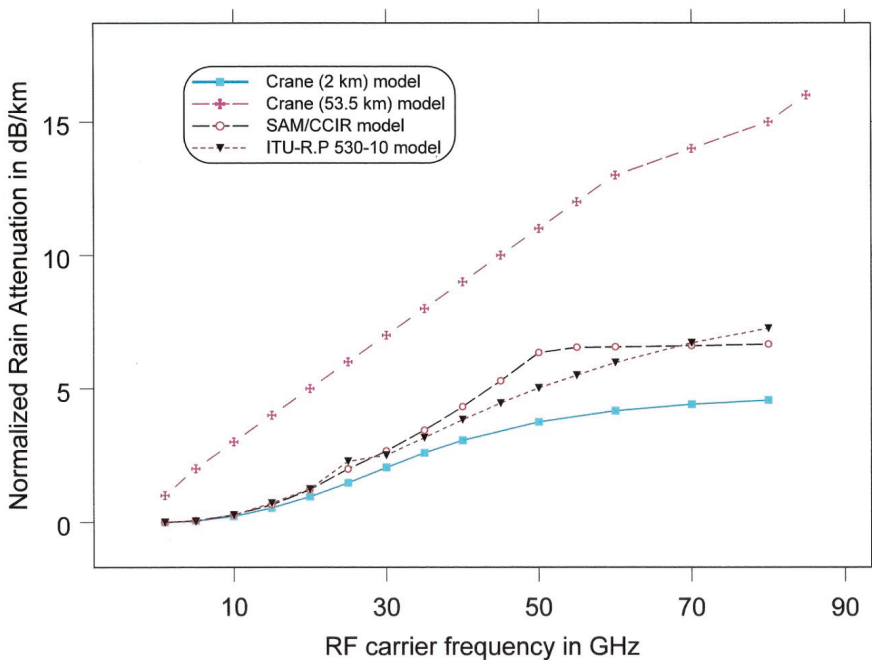


Fig. 7. Rain attenuation models at a rain rate of 15 mm/hr for vertical polarization. In general vertical polarization gives lower attenuation than horizontal polarization.

5. Links Simulation

The DWWAN links and path profiles have been simulated based on the data of a preliminary surveying of the designated regions and a terrain database integrated with the model. The model employs inputs such as: (I) system configuration signature (II) Hop and propagation Data (III) Space diversity protection has been adopted and determined by the obtained results. Diversity reception is needed only in link {L24 (24A, 24B)} and space diversity is undertaken with separation between antennas (3.0 m, $G = 38.8$ dB) as 8 m. (IV) All link performance are compared with the compliance of the ITU-T G.826 target. Path profiles have been simulated for all the 28 links with a typical profile shown in Fig. 8 for L24, which shows terrain heights and the three rays for the carrier propagation assuming an antenna clearance (1.0, 0.6, 0.6) of the first Fresnel Zone radius (F1) from the multipath propagation. The DWWAN radio link antennas are usually placed at considerable heights above ground level, to extend the radio horizon and the link range. Figure 9 (a) shows the antenna heights values as simulated from the optimum path profiling which includes intervening terrain and various propagation factors {rain precipitation is taken as 15 mm/ hour for vertical polarization}, with heights ranging between 10-95 meters. Assuming high gain single polarized antennas { $G = 37-39$ dB}, Fig. 9 (a) is also showing the number of 2.4 m and 3.0 m antennas as some nodes are having multiple links in different directions. Several iterations of the simulation have been performed until the final optimum parameters are obtained. Figure 9 (b) shows the variation of received power with the hop length for all the links. In Fig. 10 the variation of received power per channel per link is indicated with the severely errored seconds (SES) multipath-fading margin. Showing that the range of received power is {-35, -14 dBm} and the severely errored seconds (SES) fading margin range {35, 60 dB}. All the links are taken as SDH digital paths, operating at 155.52 Mbits/sec which is a trail carrying the SDH payload and associated overhead through the network between the terminating equipment.

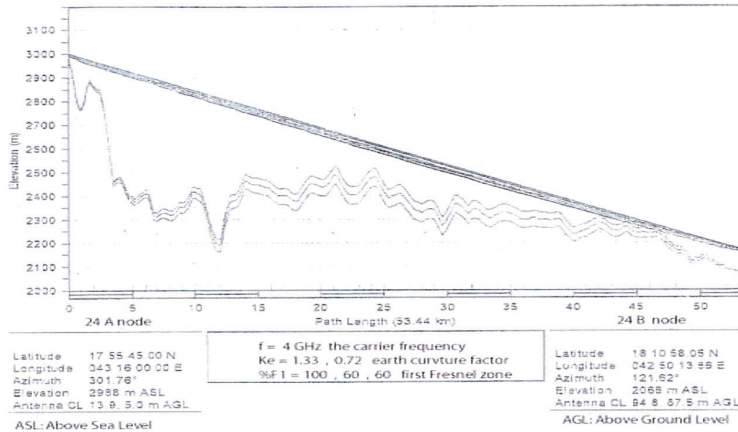


Fig.(8): The path profile of the longest link in the DWWAN between nodes 24A & 24B, showing the rugged mountain area with a height of 3000m ASL. All propagation anomalies and region climate parameters are taken into account.

Fig. 8. The path profile of the longest link in DWWAN between nodes 24A & 24B, showing the rugged mountain area with a height of 3000m ASL. All propagation anomalies and region climate parameters are taken into account.

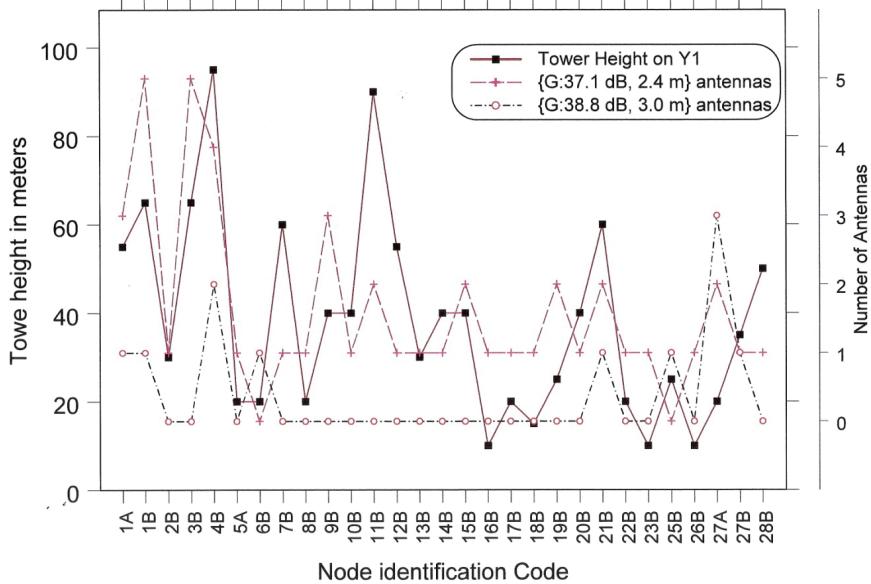


Fig. 9 (a). The various tower heights which are produced from path simulations for the different nodes, taking into account all propagation anomalies.

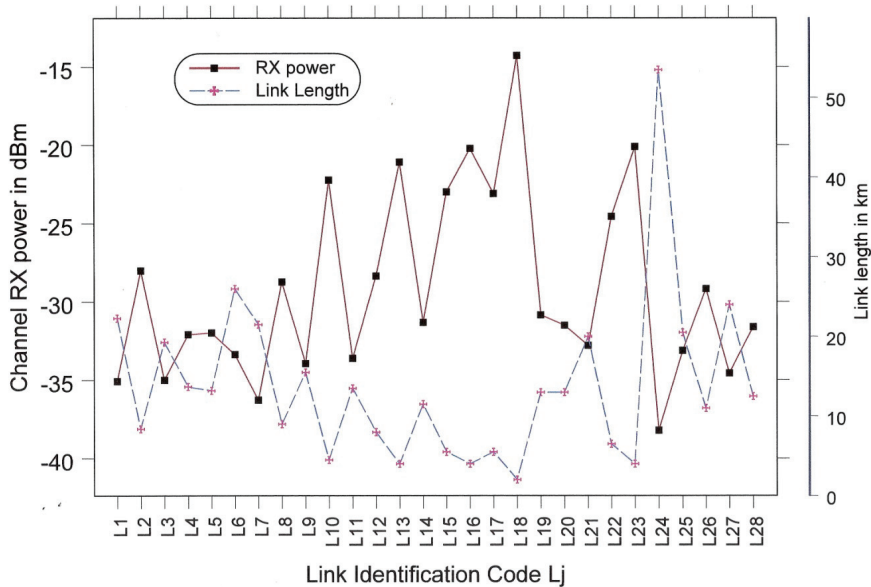


Fig. 9 (b). RX simulated power for the various links taking into account propagation anomalies and systems signature.

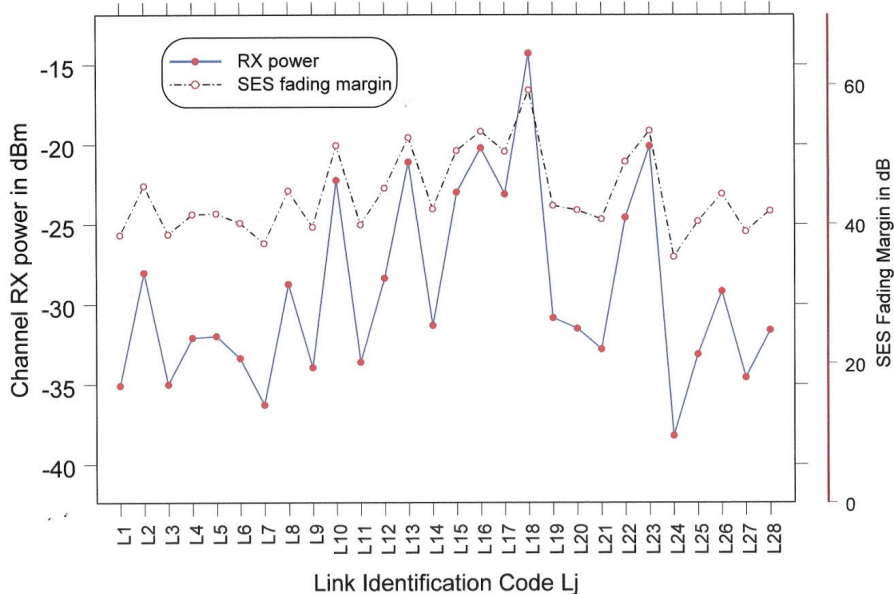


Fig. 10. The simulated RX power per channel with the severely errored seconds (SES) fading margin.

6. Conclusion

A digital wireless wide area network (DWWAN) design methodology is outlined for bands below 10 GHz, as these frequencies have very low rain attenuation and long propagation distances. Such a system is designed around the 4 GHz band that cover 56 nodes, 28 links in a rugged mountain zone with the longest link 53.44 Km. To combat the various fading mechanisms, digital microwave systems uses fixed MQAM modulation, with $M=32\dots512$, realizing SDH data rates that can reach to $\{2 \times 155.52 \text{ Mbits/sec}\}$ per single frequency pair (orthogonal beams). A proposal to employ adaptive MQAM scheme is introduced, assuming frequency non selective slowly fading channels. The symbol error rate and spectral efficiency equations of adaptive MQAM Rician fading channels are established. Adaptive modulation techniques can satisfy the growth in demand for wireless communications capacity, as the transmitted signal varies according to the instantaneous fading channel power. As a result, much higher bit rates relative to the conventional fixed signaling can be achieved. Simulations show that spectral efficiencies (SPE) up to 8.5 bits/sec/Hz at a BER = 1E-06 can be obtained for an average SNR of 32 dB., and this gives about 255 Mbits/sec for a bandwidth of 30 MHz, while the Shannon limit values are $\{\text{SPE} = 15 \text{ bits/sec/Hz, at average SNR}=33.39 \text{ dB}\}$. As the bit error rate (BER) requirement is relaxed to 1E-3 simulation shows that SPE goes higher to 9.68 bits/sec/Hz for an average SNR of 32 dB.

Simulations of the ITU performance parameters for the SDH payloads, namely the errored second ratio (ESR), severely errored second ratio (SESR) & background block error ratio (BBER) show that the designed link parameters meet the International Telecommunication Union (ITU) model target G.826.

The above DWWAN can serve as a broadband wireless utility network when integrated with SCADA stations. The SCADA net employs remote terminal units (remote processors) and Load dispatch Centers (LDC) {cluster of large number of processors or supercomputer}, this architecture provides power grid management functions covering the complex dynamic systems control and data collection.

References

- [1] **Tang, D.** and **Baker, M.**, "Analysis of a Metropolitan Area Wireless Network" *Journal of Wireless Networks*, **8**(2/3):107-120 (2000), Kluwer Academic Publishers + ACM, The Netherlands.

- [2] **Smida, B. and others,** "MC-CDMA performance evaluation over multipath Fading channel Using the characteristic function method" *IEEE Transactions on Communications*, **49(8)**: 1325-1328 (2001).
- [3] **Wang, X. and others,** "An overlapping Window Decorrelating Multiuser Detector for DS-CDMA Channels" *IEEE Transactions on Communications*, **49(8)**: 1488-1495 (2001).
- [4] **Woo So, J. and others,** "Performance Analysis of DS/SSMA unslotted ALOHA system With Variable Length Data Traffic", *IEEE Journal on Selected Areas in Communications*, **19(11)**: 2215-2224 (2001).
- [5] **Natarajan, B. and others,** "Innovative Pulse Shaping for High Performance Wireless TDMA", *IEEE Communications Letter*, **5(9)**: 372-374 (2001).
- [6] **Taylor, D.F. and Shafi, M.,** "Decision Feedback Equalization For Multipath Induced Interference In Digital Microwave LOS Links", *IEEE Transactions on Communications*, **32(3)**: 267-279 (1984).
- [7] **Annamalai, A. and Tellambura, C.,** "Error Rates for Nakagami-m Fading Multichannel Reception of Binary and M-ary Signals", *IEEE Transactions on Communications*, **49**, (1): 58-68 (2001).
- [8] **Turin., G. L. and others,** "Simulation of Urban Vehicle Monitoring Systems", *IEEE Transactions on Vehicular Tech.*, pp. 9-16, February (1972).
- [9] **Suzuki, H.,** "A statistical Model for Urban Multipath Channels with Random Delay" *IEEE Transactions on Communications*, **25**: 673-680 (1977).
- [10] **Proakis, J. G.,** "Digital Communications", McGraw-Hill Companies, Inc, USA (1995).
- [11] **Rummmler, W.D.** "A new Selective Fading Model: Application to Propagation Data", *Bell System Tech. Journal*, **58**:1037-1071 (1979).
- [12] **Adas, A. A.,** "Optical Nets Integrate Control Over Global Grids", *IEEE Computer Applications in Power*, **11**, (4): 52-56 (1998).
- [13] **Fink, D. G. and Beaty, H. W.,** editors, "Standard Handbook for Electrical Engineers" 14th edition, McGraw-Hill Companies, Inc., USA (2000).
- [14] **Kim, K II.,** Editor, "Handbook of CDMA System Design, Engineering and Optimization" Prentice-Hall PTR, Prentice-Hall, Inc, Upper Saddle River, New Jersey 07458, USA, (2000).
- [15] *ANSI J-STD-008*, "Mobile Station- Base station Compatibility Requirements for 1.8 and 2 GHz CDMA PCS" USA, March 1995.
- [16] *ITU-T Recommendation G.826*, "Series G: Transmission Systems & Media, Digital Systems & Networks" The International Telecommunication Union (ITU) – Geneva – Switzerland – Feb. 1999.
- [17] *ITU-R Recommendation P.530-8*, "Propagation Data & Prediction Methods Required for the Design of Terrestrial Line of Sight Systems" "The International Telecommunication Union (ITU) – Geneva – Switzerland – 1999.
- [18] *ITU-R Recommendation P.530-10* "Propagation Data & Prediction Methods Required for the Design of Terrestrial Line of Sight Systems", the International Telecommunication Union (ITU) – Geneva – Switzerland – 2001.
- [19] **Contract Telecommunication Engineering (CTE),** "*PATHLOSS 4.0 & 5.0 Systems*", <http://www.pathloss.com>, USA, 2009.
- [20] **Goldsmith, A. J. and Chua, S. C.,** "Variable-Rate Variable Power MQAM for Fading channels", *IEEE Transactions on Communications*, **45**, (10): 1218-1230 (1997).
- [21] **Gradshteyn., I. S. and Ryzhik, I. M.,** "Tables of Integrals, Series, and Products" translated from Russian by Alan Jeffrey, Academic Press Inc, 111 5th Avenue, New York, NY 10003, USA (1980).
- [22] **Ajose, S. O., Sadiku, M. N. and Goni, U.,** "Computation of Attenuation, Phase, Rotation, and Cross-Polarization of Radio Waves Due to Rainfall in Tropical Regions", *IEEE Transactions on Antennas & Propagation*, p. 1-5 (1995).

- [23] **Morgan, M. A.** and **Mie, K. K.**, "Finite Element Computation of Scattering by Inhomogeneous Penetratable Bodies of Revolution", *IEEE Transactions on Antennas & Propagation*, p.202-208 (1979).
- [24] **Wolf, D. de** and **Ligthart, L.**, "Multipath Effects Due to Rain at 30-50 GHz Frequency Communication Links," *IEEE Transactions on Antennas & Propagation*, **41**(8):1132-1138 (1993).
- [25] **Morgan, M. A.**, "Finite Element Computation of Microwave Scattering by Raindrops", *Radio Science Journal*, No.6:1109-1119 (1980).
- [26] **Crane, R. K.**,"*Electromagnetic Wave Propagation through Rain*", Wiley, USA (1996).
- [27] **Olsen, R. L.**, **Rogers, D. V.** and **Hodge, D. B.**, "The aR^b Relation in the Calculation of Rain Attenuation", *IEEE Transactions on Antennas & Propagation*, **26**(2): 318-329 (1978).
- [28] **Pratt, T.** and **Bostian, C. W.**, "Satellite *Communications*" John Wiley & Sons (1986).

شبكات التحكم اللاسلكية الواسعة الانتشار المستخدمة في الطاقة الكهربائية

أحمد عدس

قسم الهندسة الكهربائية وهندسة الحاسبات - كلية الهندسة
جامعة الملك عبدالعزيز - ص.ب. ٨٠٢٠٤ جدة ٢١٥٨٩
المملكة العربية السعودية
aadas@kau.edu.sa

المستخلص. تم تصميم شبكة اتصالات لاسلكية للتحكم في شبكة الطاقة الكهربائية في منطقة جبلية وعرة ، وتحتوي على ٥٦ قطبا" و ٢٨ قناة اتصال. وقد تم عمل محاكاة لهذه الشبكة باستخدام متغيرات التصميم وشمل ذلك عدد الأريالات في الأبراج و فقدان الإشارة في الممرات اللاسلكية و توهين الإشارة بالأمطار وميزانية إشارة الاتصالات. تم محاكاة الممرات اللاسلكية باستخدام قواعد معلوماتية لطبوغرافية المنطقة (منطقة عسير) مرتبطة بخطوط الطول والعرض. القنوات اللاسلكية تعطي سرعات تصل إلى ٣١١ مليون رمز ثنائي في الثانية ، وكفاءة طيفية في المجال ٥-١١ رمز ثنائي/ثانية/هرتز. ويعتبر هذا التصميم مهما لشركات الطاقة الكهربائية من ناحية الكفاءة الطيفية وسهولة تكامله مع الشبكات الخلوية.